

Enhancing Induced Strain Actuator Authority Through Discrete Attachment to Structural Elements

Z. Chaudhry* and C. A. Rogers†

Virginia Polytechnic Institute and State University, Blacksburg, Virginia 24061

In structural control, induced strain actuators are used by bonding them or embedding them in a structure. With bonded or embedded actuators used for inducing flexure, the developed in-plane force contributes indirectly through a locally generated moment. Control authority in this configuration is thus limited by actuator offset distance. In this paper, a new concept of flexural or shape control is presented, whereby induced strain actuators such as piezoelectric ceramic patches or shape memory alloys are attached to a structure at discrete points (as opposed to being bonded). This paper specifically addresses discretely attached induced strain actuators like piezoceramic and electrostrictive actuators which are available in the form of plates or patches, and includes actuator flexural stiffness considerations. This configuration is different from the bonded actuator configuration in two ways. One, because the actuator and the structure are free to deform independently, the in-plane force of the actuator can result in an additional moment on the structure and enhanced control. Second, the actuator can be offset from the structure without an increase in the flexural stiffness of the basic structure. This allows for the optimization of the offset distance to maximize control. Enhanced control is demonstrated by comparing the static response of a discretely attached actuator beam system with its bonded counterpart system. The advantage of this configuration over the bonded configuration is also verified experimentally.

Introduction

IN recent years, there has been increased interest in the use of induced strain actuators for various types of structural control. A number of models have been developed to represent the induced strain actuator and substrate coupling. Models of strain actuators coupled with simple beams¹⁻⁵ and plates^{6,7} have been introduced. Most of this work has focused on the development of accurate models to represent actuator and substrate coupling. In all of these models, however, the actuators are either embedded or bonded to the surface of the structure. No other configuration for mounting the actuator on the structure has been considered.

The focus of this research has been to investigate various configurations for integrating induced strain actuators into structures and to determine an efficient way of utilizing induced strain actuators. The conventional method of bonding induced strain actuators to the surface is certainly the easiest, but may not exploit the full capabilities of the induced strain actuators. By bonding or embedding an actuator in a structure, the actuator becomes part of the structure and as such, deforms along with it. The in-plane force of the actuator, which is the primary force exerted by the actuator on the structure, contributes only indirectly, i.e., in the development of a moment on the structure. This is because of a balancing action between the compression and tension members in the structure.⁸ The moment is a product of actuator force and actuator offset distance. Therefore, for a given available force, the actuator offset distance must be increased to increase the moment and consequently the authority of the actuator. Increasing the actuator offset distance poses two problems—it increases the flexural stiffness of the structure and it increases the stroke requirement of the actuator. This is the dilemma regarding structural control with embedded or surface-bonded actuators.

Faced with this dilemma, a new configuration in which the actuator is attached to the structure at discrete points is proposed. This configuration is fundamentally different from the bonded/embedded configuration. In this configuration, the structure and actuator between the two discrete points can deform independently, and the in-plane force of the actuator, which is dormant in the case of the bonded actuator, can cause out-of-plane displacements of the structure. Also, because now the actuator offset distance can be increased without any increase in the basic flexural stiffness of the structure (as seen by the actuator), this distance can be optimized for maximum actuator authority.

Two implementations of this concept are possible. In the first, the actuator (e.g., shape memory alloy actuator wires) does not possess any flexural stiffness and, therefore, force exerted by the induced strain actuator on the structure is directed along a straight line joining the two attachment points. This configuration is the most efficient, and results in much greater control compared to the bonded configuration. The formulation and experimental results for this configuration and its variants have already been investigated and have been reported in an earlier paper.⁹ In this paper, the second implementation, where the actuator [like piezoelectric (PZT) and electrostrictive actuators] possesses flexural stiffness, is analyzed. In this configuration, the actuator authority is again enhanced particularly due to correct selection of the actuator offset distance.

Formulation

Consider a simply supported beam with an induced strain actuator attached at two discrete points, as shown in Fig. 1. When the

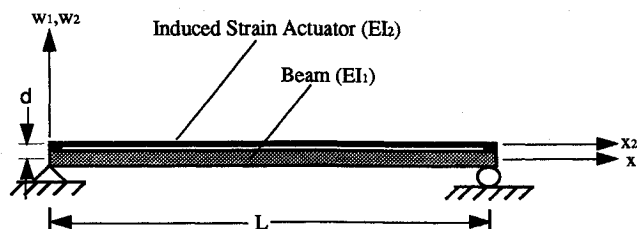


Fig. 1. Geometry of the problem.

Received Aug. 7, 1992; revision received Jan. 15, 1993; accepted for publication Jan. 15, 1993. Copyright © 1993 by Z. Chaudhry and C. A. Rogers. Published by the American Institute of Aeronautics and Astronautics, Inc., with permission.

*Graduate Research Assistant, Center for Intelligent Material Systems and Structures. Member AIAA.

†Professor, Center for Intelligent Material Systems and Structures. Member AIAA and ASME.

actuator contracts in response to an applied electric field or temperature gradient, it exerts a compressive force on the beam and the actuator itself goes into tension. The tensile force in the actuator is exactly equal and opposite the compressive force in the beam. The form of the governing equation for both the beam and actuator is:

$$EIw_{,xxxx} \pm Pw_{,xx} = 0 \quad (1)$$

The form of the solution of the previous equation is, of course, different for the actuator and the beam. For the beam, the force P is compressive and for the actuator, the force P is tensile. In general, the flexural stiffnesses EI of the beam and the actuator are also different. The solution of the differential equation for the beam is

$$w_1(x_1) = A_1 \sin kx_1 + B_1 \cos kx_1 + C_1 x_1 + D_1 \quad (2)$$

and for the actuator

$$w_2(x_2) = A_1 \sinh \bar{k}x_2 + B_2 \cosh \bar{k}x_2 + C_2 x_2 + D_2 \quad (3)$$

where

$$k = \sqrt{P/EI_1} \quad (4)$$

and

$$\bar{k} = \sqrt{P/EI_2} \quad (5)$$

The eight constants A_i , B_i , C_i , and D_i ($i=1, 2$) are solved from the following eight boundary and matching conditions:

at $x_1=0$, and $x_2=0$:

$$w_1 = w_2 = 0 \quad (6)$$

$$w_{1,x_1} = w_{2,x_2} \quad (7)$$

$$-EI_1 w_{1,xx} - EI_2 w_{2,xx} = -Pd \quad (8)$$

at $x_1=l$, and $x_2=l$:

$$w_1 = w_2 = 0 \quad (9)$$

$$w_{1,x_1} = w_{2,x_2} \quad (10)$$

$$-EI_1 w_{1,xx} - EI_2 w_{2,xx} = -Pd \quad (11)$$

Critical Buckling Load

The true input in such problems is applied electric field or free induced strain of the actuator (e.g., $\Lambda = d_{31}E$), but before addressing the question of the relationship between the free induced strain and the force P , the eigenvalue problem is analyzed. The characteristic equation for the critical buckling load can be obtained by simply setting the actuator offset distance d to zero:

$$2(1 - \cos kl \cosh \bar{k}l) + \frac{\bar{k}^2 - k^2}{k\bar{k}} \sin kl \sinh \bar{k}l = 0 \quad (12)$$

The critical buckling load, as it changes with the flexural stiffness ratio of the actuator and beam (EI_1/EI_2), is shown in Fig. 2. The critical buckling load has been normalized by EI_1/l^2 . Also, only flexural stiffness ratios greater than one are considered because in most applications the structure is stiffer than the actuator.

At higher values of flexural stiffness ratios, the value of the critical buckling load is asymptotic to $\pi^2 EI_1/l^2$, which is the critical buckling load of a column with both ends pinned. This is perfectly logical, because as the flexural stiffness ratio increases, the flexural stiffness of the actuator becomes less and less significant compared to the beam, until finally the actuator behaves like a cable (with negligible flexural stiffness) tied to the two ends of the beam.

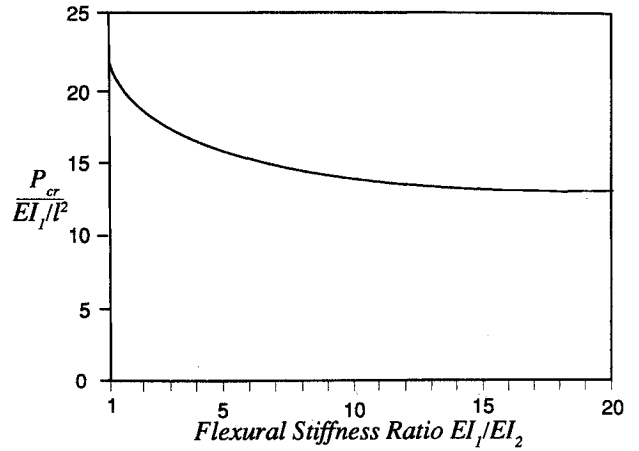


Fig. 2. Critical buckling load vs flexural stiffness ratio EI_1/EI_2 .

It is important to realize that buckling in such a configuration is possible, but for most induced strain actuators, which have limited stroke capability, it does not pose any problem. This is because catastrophic buckling (i.e., large displacements) not only requires a force greater than the critical buckling load but also requires that the force remain constant regardless of the displacement of the structure. This is of course not the case with induced strain actuators; they have limited stroke, after which they exert only a negligible force on the structure. Theoretically, buckling can take place with induced strain actuators, but displacements will still depend on the stroke capability of the actuators. Generally speaking, for any significant structural buckling, the actuator strain must be greater than 1%, which is possible only in the case of shape memory alloy (SMA) actuators. But as stated earlier, SMA actuators, which are available in the form of wires, have negligible flexural stiffness and therefore do not fall into this category of problems.

Force-Free Induced Strain Relationship

The free induced strain Λ , which is the true primary input variable, can be computed for a given force P using the following equation:

$$P = EA_2 (\epsilon_{x_2}^0 - \Lambda) \quad (13)$$

where

$$\epsilon_{x_2}^0 = \frac{du_2}{dx_2} + \frac{1}{2} \left(\frac{dw_2}{dx_2} \right)^2 \quad (14)$$

Substituting for $\epsilon_{x_2}^0$ in Eq. (13) and rearranging,

$$\frac{du_2}{dx_2} = \frac{P}{EA} - \frac{1}{2} \left(\frac{dw_2}{dx_2} \right)^2 + \Lambda \quad (15)$$

Integrating this expression yields the following expression for u_2 :

$$\begin{aligned} u_2 = & -\frac{1}{2} \left\{ \left(A_2^2 \bar{k}^2 \left(\frac{\sinh 2\bar{k}x_2}{4\bar{k}} + \frac{x_2}{2} \right) + B_2^2 \bar{k}^2 \left(\frac{\sinh 2\bar{k}x_2}{4\bar{k}} - \frac{x_2}{2} \right) \right) \right. \\ & + C_2^2 x_2 + A_2 B_2 \bar{k} \left(\frac{\cosh 2\bar{k}x_2}{2} \right) + 2A_2 C_2 \sinh \bar{k}x_2 \\ & \left. + 2B_2 C_2 \cosh \bar{k}x_2 \right\} + \left(\frac{P}{EA} + \Lambda \right) x_2 + F \end{aligned} \quad (16)$$

Two unknowns, Λ and the constant of integration F , can now be evaluated by enforcing the following two boundary conditions on the u_2 displacement at $x_2 = 0$, and $x_2 = l$ (note that at this stage the coefficients A , B , C , and D are all known):

$$u_2(0) = d w_{1,x}(0) \quad (17)$$

$$u_2(l) = d w_{1,x}(l) \quad (18)$$

From these equations, free induced strain Λ can be computed for a given force P . It is noted that the problem could have also been formulated with the free induced strain as the referenced variable instead of the force P . But since in most stability-type problems the primary variable is force, this problem was formulated accordingly.

Beam Response

With the previous equations, it is now possible to examine the beam response as a function of both the actuator-induced force P or the free induced strain Λ . Other variables that influence the response are flexural stiffness ratio EI_1/EI_2 , and actuator offset distance d .

The effect of flexural stiffness ratio on the beam response is shown in Figs. 3, 4, and 5. Figure 3 shows the response for $EI_1/EI_2 = 1$, Fig. 4 for $EI_1/EI_2 = 5$, and Fig. 5 for $EI_1/EI_2 = 10$. Although the force has been normalized by the critical buckling load (for the specified flexural stiffness ratio), it is necessary to show a different plot for each of the values of the flexural stiffness ratios because of the nonlinear relationship between force and free induced strain. In all three figures, the normalized force is plotted vs the beam center point displacement, normalized by beam length. The free induced strain corresponding to values of actuator force is plotted on the right vertical axis. For comparison, the response of the beam to a pure moment ($M = Pd$) is also plotted in each figure. Note that the

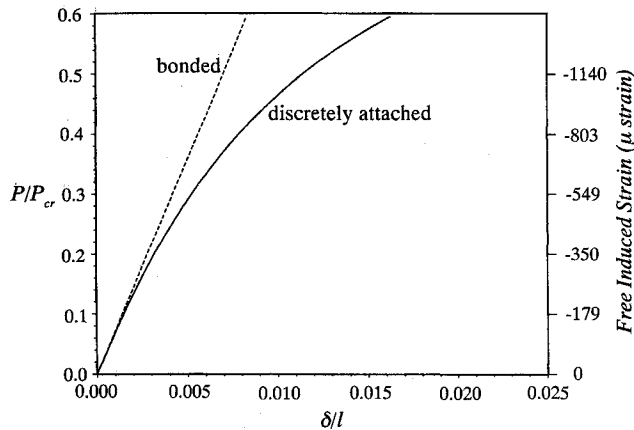


Fig. 3. Beam response for a flexural stiffness ratio = 1 ($d^* = 0.01$). The right vertical axis shows the free induced strain corresponding to the force.

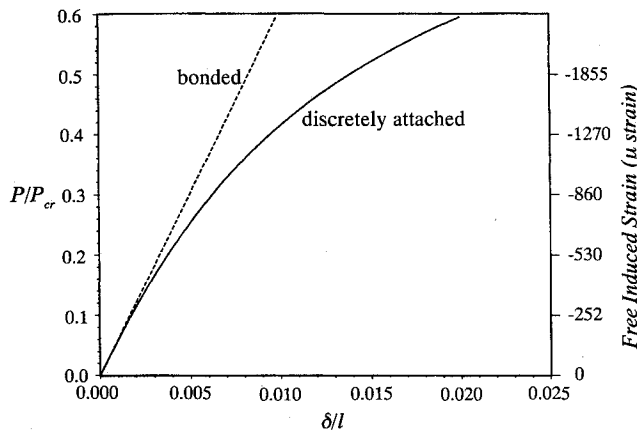


Fig. 4. Beam response for a flexural stiffness ratio = 5 ($d^* = 0.01$). The right vertical axis shows the free induced strain corresponding to the force.

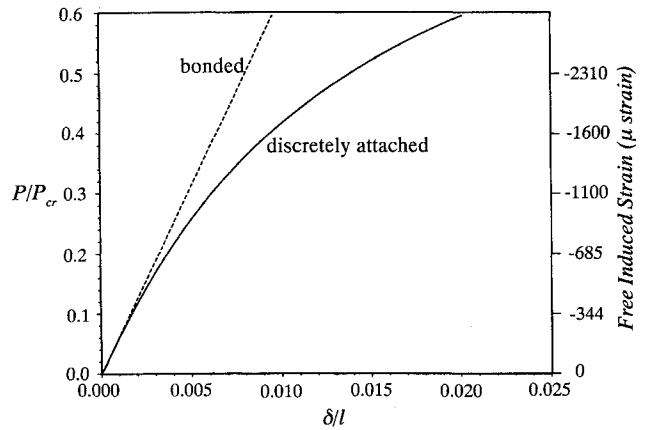


Fig. 5. Beam response for a flexural stiffness ratio = 10 ($d^* = 0.01$). The right vertical axis shows the free induced strain corresponding to the force.

free induced strain on the right vertical axis does not correspond to this linear, moment response curve.

One thing to notice from all three figures is the enhanced bending of the beam with discretely attached actuators compared to the bonded actuator case. But, to take advantage of the nonlinear region of enhanced bending, a certain minimum force and free induced strain are required. For example, in Fig. 3, where the flexural stiffness ratio is 1, a free induced strain greater than 1000 microstrain will result in approximately 70% increase in displacement, compared to that obtained with a bonded actuator.

As the flexural stiffness ratio is increased, the beam becomes stiffer compared to the actuator, and an even greater free induced strain is required to get into the nonlinear region of enhanced bending, as can be seen in Figs. 3 and 4. But, as the flexural stiffness ratio increases beyond 10, the free induced strain required to achieve a certain fraction of the critical buckling load becomes almost a constant. This is consistent with the fact that the normalized critical buckling load becomes insensitive to the flexural stiffness ratio as this ratio becomes greater than 10.

Therefore, for most practical structures, where the flexural stiffness ratio is likely to be higher than 10, an actuator with an induced strain capability of 1000 microstrain can result in a 20–30% increase in bending displacements purely due to the nonlinear effects.

Length of the beam, or distance between the two points where the actuator is attached to the structure, is also an important factor which controls the beam response. In all figures, the force P has been normalized by the critical buckling load, and the critical buckling load is inversely proportional to the length of the beam. Therefore, a longer distance between the two points where the actuator is attached to the structure reduces the critical buckling load and hence the force required to cause nonlinear effects.

Optimization of Offset Distance for Enhanced Control

Within the region of linear response, the most important parameter which influences response is the actuator offset distance. This parameter, as will be shown, if used properly can result in a substantial increase in bending control. As seen in Fig. 6 for a given value of P/P_{cr} , a higher value of the offset distance beneficially decreases the force required (from the actuator) to achieve a certain displacement, but at the same time, as seen in Fig. 7, increasing the actuator offset distance increases the stroke requirement. Mechanically when the actuator is close to the surface, the structure to which it is attached provides a greater constraint to the actuator's expansion and contraction, and in turn a greater force is developed in the actuator and applied to the structure and this leads to force saturation in the actuator. On the other hand if the actuator offset distance is increased, the constraint offered to the actuator by the structure is reduced thereby letting the actuator contract or expand more freely. And in the extreme case where there is no con-

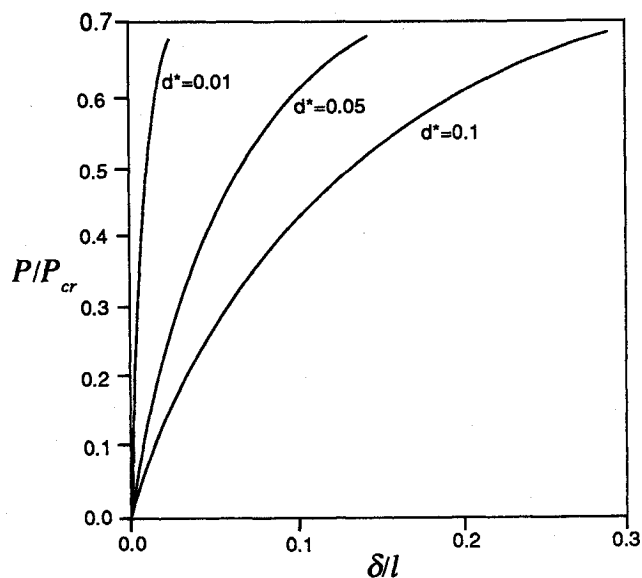


Fig. 6. Beam response for different values of the actuator offset distance d^* .

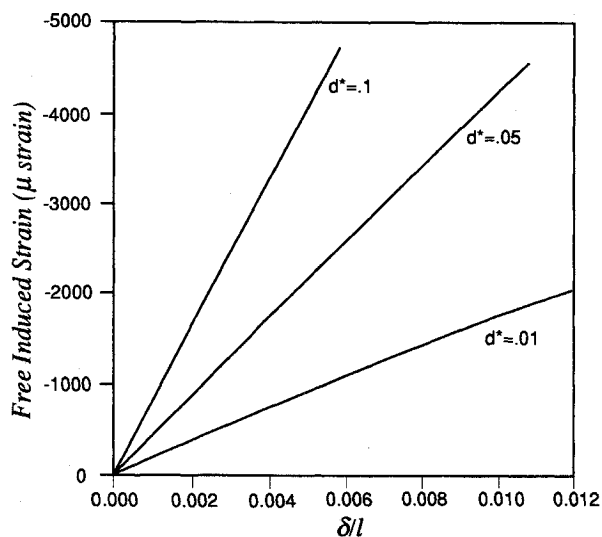


Fig. 7. Beam response for different values of the actuator offset distance d^* , showing the increased stroke requirement for higher values of actuator offset distance.

straint, it will lead to strain saturation. Between the two extremes of force saturation and strain saturation, there is in fact an optimum offset distance that maximizes the moment applied to the substrate.

To study the effect of variation of offset distance on the beam displacements, the offset distance is normalized as follows:

$$\bar{d} = d / (t_b/2)$$

and the beam displacement at the center δ is normalized by the displacement when the offset distance is a minimum, i.e., $d = 1$ or $d = t_b/2$.

$$\bar{\delta} = \delta / (\delta)_{\bar{d}=1}$$

This normalizing scheme is physically meaningful and also allows us to study the effect of variation of the offset distance in the most general manner. The minimum value of the normalized offset distance is 1 and this corresponds to when the actuator is on the surface of the beam with minimum offset distance (i.e., $d = t_b/2$). For values higher than 1, it represents the offset distance as a fraction of half of the substrate thickness. Similarly, the normalized beam

displacement represents the ratio of the beam displacements with the actuator offset to when the actuator has no offset and lies on the surface.

Figure 8 shows the normalized beam displacement plotted vs the normalized offset distance for two different values of the beam-actuator thickness ratio t_b/t_a , and $E_1/E_2 = 1$. Figure 9 shows a similar plot for $E_1/E_2 = 3$. As expected the beam displacement increases with increasing offset distance until it reaches a maximum, after which it begins to decrease again. This behavior is consistent with the physical explanation presented earlier. As seen in Fig. 8, as the substrate becomes thicker relative to the actuator the optimum offset distance also increases. As the thickness ratio is increased from 10 to 20, the normalized optimum offset distance changes from 2 to 2.6. In this figure where the modulus of the beam and the actuator are the same, the beam displacement can be increased by as much as 50% compared to bonded actuator.

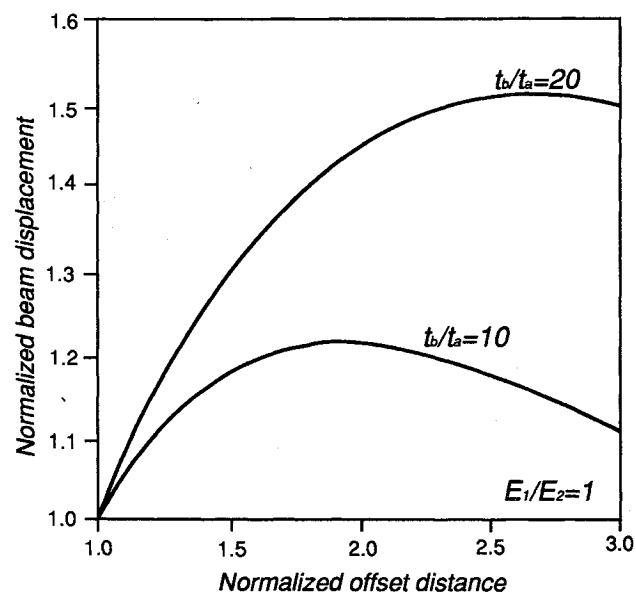


Fig. 8. Normalized beam displacement vs normalized offset distance ($E_1/E_2 = 1$) showing 1) the increased displacements with increase in actuator offset distance, and 2) the optimum offset distance.

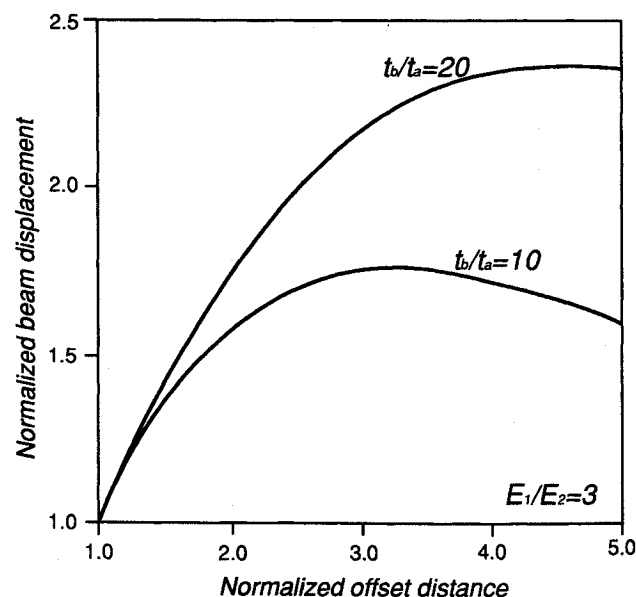


Fig. 9. Normalized beam displacement vs normalized offset distance ($E_1/E_2 = 3$) showing 1) the increased displacements with increase in actuator offset distance, and 2) the optimum offset distance.

If the substrate stiffness is greater than the actuator stiffness, the advantage of increasing the offset distance is even greater as seen in Fig. 9 where the beam-actuator modulus ratio is 3. For this stiffness ratio, optimally offsetting the actuator can result in more than 100% increase in displacements compared to bonded actuator. (It will be shown later that the bonded actuator configuration is indeed the degenerate case for this discretely attached actuator configuration.)

It is important to point out that in both Fig. 8 and 9 the beam response is in the linear region and the only factor which is changing with the change in offset distance is the moment applied to the beam (the in-plane force of the actuator does not contribute to the beam's transverse displacements). However, if the distance between the two points where the actuator is attached to the beam is long or if the force of the actuator is a significant fraction of the critical buckling load and the nonlinear effects are prominent, the optimum offset distance also becomes a function of the actuator activation level.

Relationship Between Bonded and Discretely Attached Actuator Configurations

As stated in the discussion on the optimum offset distance, the enhanced displacements in the linear region are due to the increased bending moment and not because of the nonlinear structural response. In the model for the discretely attached actuator, the beam and the actuator are subjected to concentrated moments applied at the two points where the actuator is attached to the beam. For bonded actuators, also, the action of the actuators is represented by concentrated moments applied at two ends of the actuator. Thus, in both cases the response is basically due to end moments. Then how does the discretely attached actuator formulation with minimum offset distance compare with the bonded actuator formulation? The two formulations do in fact give exactly the same response within the linear regime and the bonded configuration is a degenerate case of the discretely attached actuator configuration. In fact, it is possible to derive the Bernoulli-Euler expression for the beam curvature from considerations similar to the one used in the discretely attached formulation.¹⁰

Thus, the observations regarding the optimum offset distance can be directly applied to bonded actuators with one restriction. The restriction being that increasing the offset distance should not add to the basic flexural stiffness of the structure. This can be done by filling the area created by the offset with a foam or honeycomb type structure which only provides a filler and no increase in flexural stiffness. If the actuator offset distance is increased by increasing the basic thickness of the substrate, obviously none of the advantages mentioned previously apply because it is well known that increasing the substrate thickness increases the flexural stiffness as a square of the offset distance whereas the actuation moment increases only linearly.

The previous discussion also implies that for thinner and softer substrates it would be advantageous to embed actuators below the surface rather than surface mount them.

This problem has been specifically formulated for the case where the actuator is contracting and applying a compressive force to the beam. Within the linear region, where the response is essentially due to the concentrated end moments, all of the observations regarding the optimum offset distance also apply to a situation where the actuator is expanding and applying a tensile force to the beam. In such a situation, however, the discretely attached actuator is likely to bend itself and transmit minimal force to the structure, especially if the substrate is thick. This situation can be alleviated by having a honeycomb type filler between the actuator and the substrate. The honeycomb would ensure that the actuator itself does not bend and transfers all of the force to the substrate.

Experimental Procedure and Results

To demonstrate enhanced control experimentally a relatively thick beam was chosen. As stated earlier, increasing the offset distance is most beneficial for thicker substrates. The actuators used

were 0.25-mm-thick (10 mils) Piezoelectric Products G-1195 piezoceramic plates. A PZT patch was attached to a 1/8-in.-thick, 3/4-in.-wide, and 6-in.-long aluminum beam as shown in Fig. 10. Spacers 0.075-in. thick (which provide the optimum offset distance for this case) were placed at the two ends of the PZT to provide the necessary offset. To contrast the response of the discretely attached actuator with the bonded actuator, a second specimen with bonded PZT actuator patch was prepared. Geometric and material properties of the PZT actuator and the beam were identical for both specimen. In preparing the discretely attached actuator specimen, it was important that the actuator be absolutely straight. If there is a slight curvature, the actuator will quickly strain saturate by overcoming the slack due to the initial curvature and very little force will be transmitted to the structure.

Beam displacements were measured in the cantilever configuration at a point 1 in. from the right end of the PZT patch as shown in Fig. 10. A linear variable differential transformer (LVDT)-type miniature displacement transducer type DFG-5 (manufactured by Sangamo Schlumberger Industries), with a sensitivity of 1070 mV/mm, was used. As shown in Fig. 10, the armature of the LVDT transducer rested on the beam, and ensured positive contact between the beam and the armature at all times. The armature of the displacement transducer weighs only 1.14 g and was assumed to have negligible effect on the system response.

The dc voltage applied in the poling direction of the PZT actuator was varied from 0 to 250 V. A personal computer equipped with an analog/digital (A/D) board was used to record the voltage being applied to the actuator and the voltage output from the displacement transducer. The voltage output from the transducer was fed directly to the A/D board, but the voltage applied to the PZT was stepped down through a voltage divider and then fed to the A/D board. The applied voltage and corresponding displacements were recorded at increments of 10 V.

Figure 11 shows the results of the experiment; applied electric field is plotted on the vertical axis and displacement is on the horizontal axis. In the figure there are two sets of experimental data points, for both the bonded and the discretely attached beam-actuator specimen. Agreement between the theoretical response and the experimental data is generally good, except at high field levels, where the theoretical response overpredicts displacements.

A theoretical solution for the bonded beam-actuator specimen is obtained using the pin-force model formulation because for high beam-actuator thickness ratios, as is the case in this experiment, this model is as accurate as the Bernoulli-Euler model and simpler to use. In the computation of the theoretical response for both configurations, a strain-dependent mechanical/electrical coupling coefficient d_{31} is used. The method suggested by Crawley and Lazarus⁶ is used to compute d_{31}^* (secant definition of d_{31}). The following second-order curve fit of the reported experimental data was used to compute the value of d_{31}^* iteratively:

$$d_{31}^* = 200 + 0.0012\varepsilon - 2\varepsilon^2$$

It is important to recognize that the nonlinearity in the response in Fig. 2 is not due to structural nonlinearity but is completely due to the nonlinear field-strain behavior of the PZT actuator.

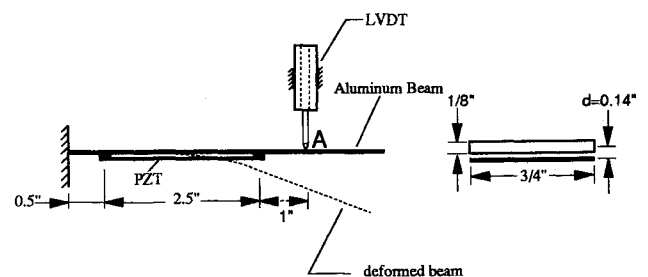


Fig. 10. Schematic representation of discretely attached beam actuator specimen and experimental setup used to measure displacements.

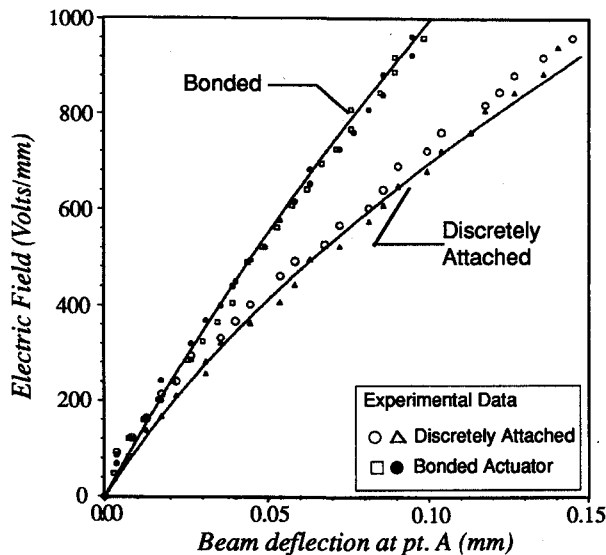


Fig. 11. Experimental results: comparison of bonded and discretely attached actuator configurations.

Table 1 Comparison of experimental and theoretical results

Type	Field, V/mm	d_{31} , pm/V	Displacement, mm		Predicted moment, in. lb	
			Predicted	Data	force, lb	
Discretely Attached	500	273	0.0646	0.0605	4.7	0.611
	1000	349	0.1640	0.1450	11.8	1.534
Bonded	500	223	0.0451	0.0445	6.16	0.3853
	1000	249	0.1000	0.1050	13.767	0.86

It is interesting to note the predicted force in the actuator at different field levels and the resulting moment applied to the beam-actuator structure. Results of the predictions for some representative values are shown in Table 1. At 1000 V/mm, the predicted force in the discrete actuator is 16% less than the bonded actuator, but the moment is 40% greater. The difference in values of d_{31} used for predicting the response of the bonded actuator and the discretely attached actuator is also apparent. With an offset piezoelectric actuator, structural control authority is enhanced as a result of the nonlinear field-strain relationship of PZT.

Conclusions

To increase the realm of applications of induced strain actuators beyond vibration control and micropositioning, it is necessary to examine configurations other than the standard bonded/embedded configuration. In this paper, a new configuration of discretely attached induced strain actuators to enhance structural control is developed and verified experimentally. As a first step, a simple beam-actuator system is analyzed. Aside from the distance between the two discrete points where the actuator is attached to the beam, the beam response is basically a function of two variables—the ratio of the flexural stiffnesses of the beam and actuator and the actuator offset distance.

This proposed configuration can enhance the response above that of the bonded actuator configuration by two mechanisms. One is by taking advantage of the geometrically nonlinear enhanced

structural response. For most practical structures where the beam actuator flexural stiffness ratio is greater than 10, this would require an actuator with a free induced capability greater than 1000 microstrain. The second mechanism is that of optimally increasing the distance through which the actuator is offset from the structure at the two points of attachment. This mechanism enhances control in both the linear and nonlinear regions of structural response and does not require any minimum stroke capability of the actuator.

The increase in actuator authority achieved by offsetting the actuator depends on the beam-actuator thickness and modulus ratio. For thicker or high modulus substrates, optimal increase in the actuator offset distance results in a substantial increase in flexural control. In experimental work with PZT actuators and aluminum beams, a 40% increase in displacements over the bonded configuration was observed.

The geometry presented in this paper is just one of the possible configurations of discretely attached actuators. Note that as soon as the constraint that the actuator be bonded to the structure everywhere (without significantly modifying the overall geometry of the structure) is relaxed, a whole array of new geometric and kinematic possibilities is opened. The concept can easily be extended to any type of actuator including magnetostrictive and PZT stacks.

Acknowledgments

The support of National Science Foundation through the Presidential Young Investigator Program (Grant MSS-9157080) and the Office of Naval Research (Grant ONR 0014-92-J-1170) is gratefully acknowledged.

References

- Forward, R. L., and Swigert, C. J., "Electronic Damping of Orthogonal Bending Modes in a Cylindrical Mast Theory," *Journal of Spacecraft and Rockets*, Vol. 17, No. 1, 1981, pp. 5–10.
- Hanagud, S., Obal, M. W., and Calise, A. J., "Optimal Vibration Control by the Use of Piezoceramic Sensors and Actuators," *Proceedings of the 28th SDM Conference* (Monterey, CA), April 1987, AIAA, Washington, DC, pp. 987–997 (AIAA Paper 87-0959).
- Crawley, E. F., and de Luis, J., "Use of Piezoelectric Actuators as Elements of Intelligent Structures," *AIAA Journal*, Vol. 25, No. 10, 1987, pp. 1373–1385.
- Bailey, T., and Hubbard, J. E., "Distributed Piezoelectric-Polymer Active Vibration Control of a Cantilever Beam," *Journal of Guidance, Control, and Dynamics*, Vol. 8, No. 5, 1985, pp. 605–611.
- Lin, M. W., and Rogers, C. A., "Analysis of a Beam Structure with Induced Strain Actuators Based on an Approximated Linear Shear Stress Field," *Proceedings of the Conference on Recent Advances in Adaptive and Sensory Materials and Their Applications*, Virginia Polytechnic Institute and State Univ., Blacksburg, Virginia, Technomic Publishing Co., Inc., Lancaster, PA, April 27–29, 1992, pp. 363–376.
- Crawley, E. F., and Lazarus, K. B., "Induced Strain Actuation of Isotropic and Anisotropic Plates," *AIAA Journal*, Vol. 29, No. 6, 1989, pp. 944–951.
- Wang, B. T., and Rogers, C. A., "Modelling of Finite Length Spatially Distributed Induced Strain Actuators for Laminate Beams and Plates," *Proceedings of the 32nd SDM Conference* (Baltimore, MD), AIAA, Washington, DC, April 1991, pp. 1511–1520 (AIAA Paper 91-1258).
- Chaudhry, Z., and Rogers, C. A., "Response of Composite Beams to an Internal Actuator Force," *Proceedings of the 32nd SDM Conference* (Baltimore, MD), AIAA, Washington, DC, April 1991, pp. 184–193 (AIAA Paper 91-1168).
- Chaudhry, Z., and Rogers, C. A., "Bending and Shape Control of Beams using SMA Actuators," *Journal of Intelligent Material Systems and Structures*, Vol. 2, No. 4, 1991, pp. 581–602.
- Chaudhry, Z., and Rogers, C. A., "A Mechanics Approach to Induced Strain Actuation of Structures," *Proceedings Third International Conference on Adaptive Structures* (San Diego, CA), Nov. 11–14, 1992, Tech-